JPL E-7402


**A. Kahraman**[1]
Research Associate.

**H. Nevzat Ozguven**[2]
Visiting Professor.
Mem. ASME

**D. R. Houser**
Professor.
Mem. ASME

Gear Dynamics and Gear Noise Research Laboratory,
Department of Mechanical Engineering,
The Ohio State University,
Columbus, OH 43210

**J. J. Zakrajsek**
Mem. ASME
National Aeronautics and Space Administration,
Lewis Research Center,
Cleveland, OH 44135


# Dynamic Analysis of Geared Rotors by Finite Elements


*A finite element model of a geared rotor system on flexible bearings has been developed. The model includes the rotary inertia of shaft elements, the axial loading on shafts, flexibility and damping of bearings, material damping of shafts and the stiffness and the damping of gear mesh. The coupling between the torsional and transverse vibrations of gears were considered in the model. A constant mesh stiffness was assumed. The analysis procedure can be used for forced vibration analysis of geared rotors by calculating the critical speeds and determining the response of any point on the shafts to mass unbalances, geometric eccentricities of gears, and displacement transmission error excitation at the mesh point. The dynamic mesh forces due to these excitations can also be calculated. The model has been applied to several systems for the demonstration of its accuracy and for studying the effect of bearing compliances on system dynamics.*


## Introduction

Even though there have been numerous studies on both rotor dynamics and gear dynamics, the studies on geared rotor dynamics have been rather recent. The study of the dynamic behavior of geared rotor systems usually requires the coupling between torsional and transverse vibration modes to be included in the model, although this is not a problem for rotors without gears.

Although several modeling and solution techniques such as lumped mass models and the use of the transfer matrix method have been applied to rotor dynamics problems, the finite element method seems to be a highly efficient way for modeling such systems. In one of the early examples of the finite element method, Nelson and McVaugh (1976) used a Rayleigh beam finite element including the effects of the translational and rotary inertias, gyroscopic moments, and the axial load. The work of Zorzi and Nelson (1977) was the generalization of the previous study (Nelson and McVaugh, 1976) to include internal damping. Later, Nelson (1980) developed a Timoshenko beam by adding shear deformation to the Rayleigh beam theory. This model was extended by Ozguven and Ozkan (1983) to include effects such as transverse and rotary inertia, gyroscopic moments, axial load, internal hysteretic and viscous damping, and shear deformations in a single model. None of the models described above can handle geared rotor systems, although they are capable of determining the dynamic behavior of rotors which consist of a shaft supported at several points and carrying rigid disks at several locations.

Gear dynamics studies, on the other hand, have usually neglected the lateral vibrations of the shafts and bearings, and have typically represented the system with a torsional model. Although neglecting lateral vibrations might be a good approximation for systems having shafts with small compliances, it was observed experimentally (Mitchell and Mellen, 1975) that the dynamic coupling between the transverse and torsional vibrations due to the gear mesh affects the system behavior considerably when the shafts have high compliances. This fact directed the attention of investigators to the inclusion of lateral vibrations of the shafts and the bearings in mathematical models. Lund (1978) developed influence coefficients at each gear mesh by using the Holzer method for torsional vibrations and the Myklestad-Prohl method for lateral vibrations. He obtained critical speeds and a forced vibration response by coupling the results of these two methods. Hamad and Seireg (1980) studied the whirling of geared rotor systems supported on hydrodynamic bearings. Torsional vibrations were not considered in this model and the driven shaft was assumed to be rigid. Iida et al. (1980) considered the same problem by taking one of the shafts to be rigid and neglecting the compliance of the gear mesh, and obtained a three degree of freedom model to determine the first three vibration modes and the forced vibration response due to the unbalance and the geometric eccentricity of one of the gears. They also reported that their theoretical results confirmed experimental measurements. Later, Iida et al. (1984, 1985, 1986) applied their model to a larger system which consists of three shafts

[1]Currently with the General Motors Research Laboratories, Power Systems Research Department, 30500 Mound Road, Warren, MI 48090-9055.
[2]Currently with the Middle East Technical University, Ankara, Turkey.


Contributed by the Power Transmission and Gearing Committee for publication in the JOURNAL OF MECHANICAL DESIGN. Manuscript received April 1989. Associate Technical Editor: D. G. Lewicki.

coupled by two gear meshes. Hagiwara et al. (1981) developed a simple model that includes the transverse flexibilities of the shafts by using discrete stiffness values, and studied the forced response of geared shafts due to unbalances and runout errors. They took the damping and compliances of the journal bearings into account and assumed the mesh stiffness to be constant.

Another approach in the study of gear dynamics has been to use transfer matrix methods. In most of these studies the mesh stiffness was taken to be periodic. Daws (1979) developed a three-dimensional model considering the mesh stiffness as a time varying three-dimensional stiffness tensor. He included the force coupling due the interaction of gear deflection and time varying stiffness, whereas, he neglected the dynamic coupling in the model. As a continuation of this study, Mitchell and David (1985) showed that dynamic coupling terms were dominant on the dynamic behavior of the system. Iwatsubo et al. (1984a) also used the transfer matrix method in their models and calculated the force response due to mass unbalance only for a constant mesh stiffness. Later, they (1984b) included the effects of periodic variation of mesh stiffness and profile errors of both gears.

Neriya et al. (1984) extended the model of Iida et al. (1980) by representing a single gear by a two mass, two spring, two damper system which used a constant mesh stiffness. The shafts were assumed massless and equivalent values for the lateral and torsional stiffnesses of shafts were used to obtain a discrete model. Later Neriya et al. (1985) employed the finite element method in finding the dynamic behavior of geared rotors. They also found the forced vibration response of the system due to mass unbalances and runout errors of the gears by using modal summation. Bagci and Rajavenkateswaran (1987) used spatial finite line-element technique to perform mode shape and frequency analysis of coupled torsional, flexural and longitudinal vibratory systems with special application to multicylinder engines. They concluded that coupled torsional and flexural modal analysis is the best procedure to find natural frequencies and corresponding mode shapes. An extensive survey of mathematical models used in gear dynamics analyses is given in a recent paper by Ozguven and Houser (1988a).

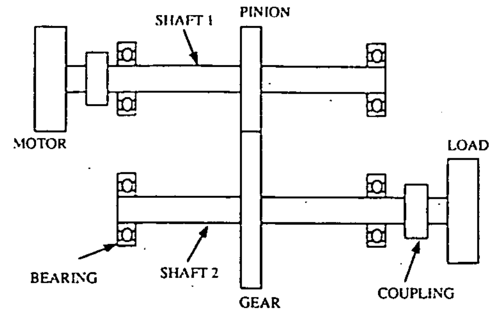


**Fig. 1 A typical gear-rotor system**

The objective of this study was to develop a finite element program for the dynamic analysis of geared rotor systems and to study the effect of bearing flexibility, which is usually neglected in simpler gear dynamics models, on the dynamics of the system. In the formulation of rotor elements, except for gears, the rotor dynamics program ROT-VIB which has been developed in a previous study (Ozguven and Ozkan, 1983; Ozkan, 1983) was used. However, due to the coupling between torsional and transverse vibration modes, a torsional degree of freedom has been added to the formulation, and some special features of ROT-VIB have been omitted.

## Theory

A typical geared rotor system is shown in Fig. 1. The system consists of a motor connected to one of the shafts by a coupling, a load at the other end of the other shaft, and a gear pair which couples the shafts. Both shafts are supported at several locations by bearings. Hence, a geared rotor system consists of the following elements:

(*a*) shafts,
(*b*) rigid disks,
(*c*) flexible bearings,
(*d*) gears.

When two shafts are not coupled, each gear can be modeled as

## Nomenclature

$[C]$ = damping matrix of the system
$c_m$ = mesh damping coefficient
$[C_m]$ = mesh damping matrix
$c_s$ = modal damping value of $s$th mode
$d_1, d_2$ = diameters of driving and driven shafts, respectively
$e_g, e_p$ = geometric eccentricities of the gear and the pinion, respectively
$e_t$ = amplitude of the static transmission error excitation
$F_s$ = average value of force transmitted (static load)
$\{\mathbf{F}_t\}$ = total force vector of the system
$i$ = unit imaginary number
$I_g, I_p$ = mass moment of inertias of the gear and the pinion, respectively
$J_d, J_m$ = mass moment of inertias of load and motor, respectively
$k_m$ = mesh stiffness coefficient
$[K_m]$ = mesh stiffness matrix
$K_{tcl}$ = torsional compliance of the flexible coupling
$k_{xx}, k_{yy}$ = bearing stiffness values
$L_1, L_2$ = lengths of driving and driven shafts, respectively
$m_g, m_p$ = masses of the gear and the pinion, respectively
$M_1, M_2$ = moments due to the dynamic mesh forces
$N_p$ = tooth number of driving gear
$\{\mathbf{q}\}$ = total response of the system
$r_g, r_p$ = base circle radii of the gear and the pinion, respectively
$t$ = time
$U_g, U_p$ = mass unbalances of the gear and the pinion, respectively
$W_1, W_2$ = dynamic mesh forces
$x_g, x_p$ = coordinates perpendicular to the pressure line at the centers of the gear and the pinion, respectively
$y_g, y_p$ = coordinates in the direction of the pressure line at the centers of the gear and the pinion, respectively
$[\alpha]$ = dynamic compliance matrix
$\theta_2, \theta_1$ = total angular rotations of the gear and the pinion, respectively
$\theta_p, \theta_g$ = fluctuating parts of $\theta_1$ and $\theta_2$, respectively
$\omega_p, \omega_g$ = rotational speeds of driving and driven shafts, respectively
$\omega_r$ = $r$th natural frequency
$[\Phi]$ = modal matrix
$\{\Phi^s\}$ = $s$th normalized eigen vector
$\zeta_s$ = modal damping coefficient for the $s$th mode

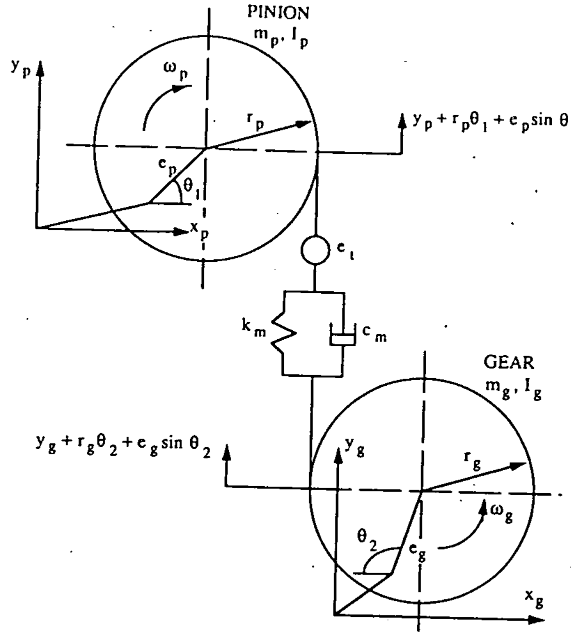


Fig. 2 Modeling of a gear mesh

a rigid disk. However, when they are in mesh, these rigid disks are connected by a spring-damper element representing the mesh stiffness and damping.

For the formulation of the first three types of elements listed above, the existing program ROT-VIB, (Ozguven and Ozkan, 1983) was used. ROT-VIB is a general purpose rotor dynamics program which can calculate whirl speeds, corresponding mode shapes, and the unbalance response of shaft-rigid disk-bearing systems by including the effects of rotary and transverse inertia, shear deformations, internal hysteretic and viscous damping, axial load and gyroscopic moments. In ROT-VIB, the classical linearized model with eight spring and damping coefficients are used for modeling bearings, and finite elements with four degrees of freedom at each node (excluding axial motion and torsional rotation) are employed for the shaft elements.

In the present analysis, the formulation used in ROT-VIB for these elements was employed with some modifications. First, in order to avoid nonsymmetric system matrices which result in a complex eigenvalue problem, the gyroscopic moment effect was ignored and the internal damping of the shafts was included only in the damping matrix. Second, the gear mesh causes coupling between the torsional and transverse vibrations of the system, which makes it necessary to include the torsional degree of freedom. Therefore, the mass and stiffness matrices of the system which are taken from ROT-VIB have been expanded in the new model to include the torsional motion of the shafts. Hence, five degrees of freedom have been defined at each node with only axial motion being excluded. The axial motion, which would be important for helical gears, could easily be included in subsequent analyses.

**Gear Mesh Formulation.** A typical gear mesh can be represented by a pair of rigid disks connected by a spring and a damper along the pressure line which is tangent to the base circles of the gears as shown in Fig. 2. In this model, the mesh stiffness and damping values are assumed to be constant. The tooth separation is not considered since the gears are assumed to be heavily loaded. By choosing the $y$ axis on the pressure line and the $x$ axis perpendicular to the pressure line, the transverse vibrations in the $x$ direction are uncoupled from both the torsional vibrations and the transverse vibrations in the $y$ direction, provided negligible mesh friction. For the system of Fig. 2, the dynamic mesh forces in the $y$ direction can be written as

$$W_1 = c_m(\dot{y}_p + r_p\dot{\theta}_1 + e_p\omega_p\cos\theta_1 - \dot{y}_g - r_g\dot{\theta}_2 - e_g\omega_g\cos\theta_2 - e_t N_p\omega_p\cos(N_p\theta_1)) + k_m(y_p + r_p\theta_1 + e_p\sin\theta_1 - y_g - r_g\theta_2 - e_g\sin\theta_2 - e_t\sin(N_p\theta_1)); \quad (1)$$

$$W_2 = -W_1; \quad (2)$$

where $W_1$ and $W_2$ are mesh forces in the $y_p$ and $y_g$ directions at the pinion and the gear locations respectively. Here, $c_m$ and $k_m$ are mesh damping and mesh stiffness values, $e_p$ and $e_g$ are geometric eccentricities of the pinion and the gear, and $r_p$ and $r_g$ are base circle radii of the pinion and the gear. The angles $\theta_1$ and $\theta_2$ are the total angular rotations of the pinion and the gear, respectively, and are equal to

$$\theta_1 = \theta_p + \omega_p t; \quad \theta_2 = \theta_g + \omega_g t \quad (3,4)$$

where $\theta_p$ and $\theta_g$ are the alternating parts of rotations and $\omega_p$ and $\omega_g$ are the spin speeds of the driving and driven shafts, respectively. The displacement $e_t$ which may be considered to be a transmission error excitation, is applied at the mesh point. This displacement is usually taken to be sinusoidal at the gear mesh frequency, but one could include higher harmonics also. It has been shown by Ozguven and Houser (1988b) that it is possible to simulate the variable mesh stiffness approximately, by using a constant mesh stiffness with a displacement excitation representing the "loaded" static transmission error. Thus, by choosing $e_t$ as the amplitude of the loaded static transmission error, the effect of the variable mesh stiffness can be approximately considered in the model.

Mesh forces also cause moments about dynamic centers of the gears which are equal to

$$M_1 = W_1(r_p + e_p\cos\theta_1); \quad M_2 = W_2(r_g + e_g\cos\theta_2) \quad (5,6)$$

Here, the initial angular position of geometric eccentricities are taken to be zero. The mesh stiffness and damping matrices and the force vector of the system due to gear errors and unbalances can be obtained by writing the force transmitted as the summation of the average transmitted force (static load), $F_s$, and a fluctuating component, and then neglecting high order terms following the substitution of equations (1) and (2) into equations (5) and (6). Defining the degrees of freedom of the system at which the gear coupling effect appears, as

$$\{\mathbf{q}_1\} = \lfloor y_p\ \theta_p\ y_g\ \theta_g \rfloor^T \quad (7)$$

the additional mesh stiffness matrix which causes the coupling effect and corresponds to $\{\mathbf{q}_1\}$ can be obtained from equations (1), (2), (5), and (6) to be

$$[K_m] = \begin{bmatrix} k_m & k_m r_p & -k_m & -k_m r_g \\ k_m r_p & k_m r_p^2 & -k_m r_p & -k_m r_p r_g \\ -k_m & -k_m r_p & k_m & k_m r_g \\ -k_m r_g & -k_m r_p r_g & k_m r_g & k_m r_g^2 \end{bmatrix}. \quad (8)$$

Similarly, the mesh damping matrix can be found to be

$$[C_m] = \begin{bmatrix} c_m & c_m r_p & -c_m & -c_m r_g \\ c_m r_p & c_m r_p^2 & -c_m r_p & -c_m r_p r_g \\ -c_m & -c_m r_p & c_m & c_m r_g \\ -c_m r_g & -c_m r_p r_g & c_m r_g & c_m r_g^2 \end{bmatrix}. \quad (9)$$

The other degrees of freedom defined at nodes $p$ and $g$ have not been included in the vector $\{\mathbf{q}_1\}$ since elements of $[K_m]$ and $[C_m]$ corresponding to these degrees of freedom are all zero. For the degrees of freedom expressed as

Table 1 Parameters of the system shown in Fig. 1

| | | | |
|---|---|---|---|
| $J_m$ | : 0.459 Kg-m$^2$ | $d_1$ | : 0.03 m |
| $J_d$ | : 0.549 Kg-m$^2$ | $d_2$ | : 0.02 m |
| $I_p$ | : 0.030 Kg-m$^2$ | $e_g$ | : $1.2\times10^{-5}$ m |
| $I_g$ | : $6.28\times10^{-3}$ Kg-m$^2$ | $U_g$ | : $2.8\times10^{-4}$ Kg-m |
| $m_p$ | : 16.96 Kg | $e_p$ | : 0.0 |
| $m_g$ | : 5.65 Kg | $U_p$ | : 0.0 |
| $r_p$ | : 0.1015 m | $e_t$ | : 0.0 |
| $r_g$ | : 0.0564 m | $K_{tc1}$ | : 115.0 N-m/rad |
| $L_1$ | : 0.78 m | $k_m$ | : $2.0\times10^8$ N/m |
| $L_2$ | : 0.40 m | | |

$$\{\mathbf{q}_2\} = [y_p\ x_p\ \theta_p\ y_g\ x_g\ \theta_g]^T \tag{10}$$

the force vector due to the gear runouts, the static transmission error, and the gear mass unbalances $U_p$ and $U_g$ is given by

$$\{\mathbf{F}\} = \begin{Bmatrix} U_p\omega_p^2\sin\omega_p t + F_1 \\ U_p\omega_p^2\cos\omega_p t \\ -F_s e_p\cos\omega_p t + r_p F_1 \\ U_g\omega_g^2\sin\omega_g t - F_1 \\ U_g\omega_g^2\cos\omega_g t \\ F_s e_g\cos\omega_g t - r_g F_1 \end{Bmatrix} \tag{11}$$

where

$$F_1 = c_m(e_g\omega_g\cos\omega_g t - e_p\omega_p\cos\omega_p t + e_t N_p\omega_p\cos(N_p\omega_p t)) + k_m(e_g\sin\omega_g t - e_p\sin\omega_p t + e_t\sin(N_p\omega_p t)) \tag{12}$$

Adding the mesh stiffness matrix given by equation (8) to the stiffness matrix of the uncoupled rotor system yields the total stiffness matrix of the system. The natural frequencies $\omega_r$ and the mode shapes $\{\mathbf{u}^r\}$ of the system can be determined by solving the governing eigenvalue problem. In the solution, the Sequential Threshold Jacobi method was used.

**Forced Response.** The total force vector is obtained by combining the force vector due to the mass unbalances of the shafts and the other disks and the force vector due to the mass unbalances of gears and gear errors as given in equation (11). This vector is the sum of harmonic components with three different frequencies $\omega_p$, $\omega_g$ and $(N_p\omega_p)$, and has the following general form

$$\{\mathbf{F}_t\} = \{\mathbf{F}_{sp}\}\sin\omega_p t + \{\mathbf{F}_{cp}\}\cos\omega_p t + \{\mathbf{F}_{sg}\}\sin\omega_g t + \{\mathbf{F}_{cg}\}\cos\omega_g t + \{\mathbf{F}_{sm}\}\sin(N_p\omega_p t) + \{\mathbf{F}_{cm}\}\cos(N_p\omega_p t) \tag{13}$$

The total response of the system due to this excitation can be written as

$$\{\mathbf{q}\} = [\alpha_p]\{\mathbf{F}_{sp}\}\sin\omega_p t + [\alpha_p]\{\mathbf{F}_{cp}\}\cos\omega_p t + [\alpha_g]\{\mathbf{F}_{sg}\}\sin\omega_g t + [\alpha_g]\{\mathbf{F}_{cg}\}\cos\omega_g t + [\alpha_m]\{\mathbf{F}_{sm}\}\sin(N_p\omega_p t) + [\alpha_m]\{\mathbf{F}_{cm}\}\cos(N_p\omega_p t) \tag{14}$$

where $[\alpha_p]$, $[\alpha_g]$ and $[\alpha_m]$ are the dynamic compliance matrices corresponding to the excitation frequencies, $\omega_p$, $\omega_g$ and $(N_p\omega_p)$, respectively, and given by

$$[\alpha_p] = \sum_{s=1}^{n} \frac{\{\Phi^s\}\{\Phi^s\}^T}{(\omega_s^2 - \omega_p^2 + i\omega_p c_s)}; \tag{15}$$

$$[\alpha_g] = \sum_{s=1}^{n} \frac{\{\Phi^s\}\{\Phi^s\}^T}{(\omega_s^2 - \omega_g^2 + i\omega_g c_s)}; \tag{16}$$

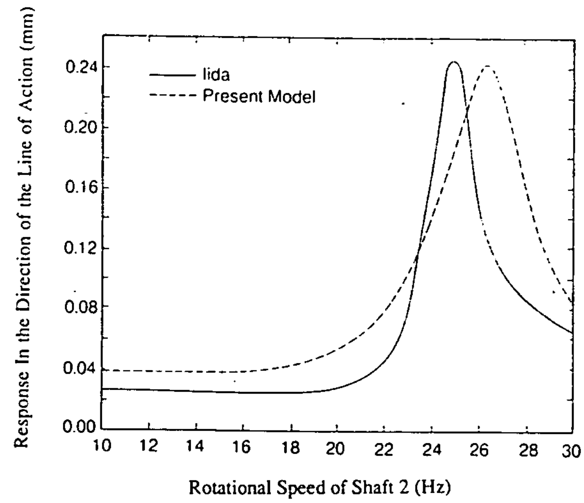


**Fig. 3 Comparison of the theoretical values of the dynamic deflection of the driven gear in the pressure line direction with the experimental results given by Iida et al. (1980)**

$$[\alpha_m] = \sum_{s=1}^{n} \frac{\{\Phi^s\}\{\Phi^s\}^T}{(\omega_s^2 - N_p^2\omega_p^2 + iN_p\omega_p c_s)}. \tag{17}$$

Here, $\{\Phi^s\}$ represents the $s$th mass matrix normalized modal vector, $n$ is the total number of the degrees of freedom of the system, $i$ is the unit imaginary number, and $c_s$ is the $s$th modal damping value given by the $s$th diagonal element of the transformed damping matrix $[\bar{C}]$ where

$$[\bar{C}] = [\Phi]^T[C][\Phi] \tag{18}$$

and $[\Phi]$ is the normalized modal matrix. In this approach it is assumed that the damping matrix is the proportional type, which is usually not correct for such systems. When the damping is not proportional, the transformed damping matrix $[\bar{C}]$ will not be diagonal in which case $c_s$ will still be the $s$th diagonal element and all nonzero off-diagonal elements are simply ignored when using the classical uncoupled mode superposition method. Another approach for including damping in the dynamic analysis of such systems would be assuming a modal damping, $\zeta_s$, for each mode and then replace $c_s$ in equations (15) to (17) by $2\zeta_s\omega_s$. However, it is believed that using the actual values for damping, when they are known, and employing an approximate solution technique may result in more realistic predictions than assuming a modal damping value for each mode.

## Applications and Numerical Results

**Comparison with an Experimental Study.** As the first application, the experimental set-up of Iida et al. (1980) has been modeled. As shown in Fig. 1, the system consists of two geared rotors, one is connected to a motor with a mass moment of inertia of $J_m$ and the other is connected to a load with a mass moment of inertia of $J_d$. Each shaft is supported by a pair of ball bearings. The parameters of the system are listed in Table 1. The gears with inertias $I_p$ and $I_g$ are both mounted on the middle of the shafts of lengths $L_1$ and $L_2$ and diameters $d_1$ and $d_2$, respectively. In their study, Iida et al. (1980) did not specify the length of the second shaft, $L_2$, and the properties of bearings and couplings. Instead they gave the total torsional stiffness values for driving and driven parts of the system and a total transverse stiffness value for the second shaft. Therefore, the length of the second shaft, $L_2$, and the torsional stiffness of the first coupling, $K_{tc}1$, have been estimated so that the total values given by Iida et al. (1980) were obtained. The forced vibration response due to the

Table 2 Parameters of the system shown in Fig. 4

| | |
|---|---|
| $J_m$ : $1.15\times10^{-2}$ Kg-m² | $r_p$ : 0.047 m |
| $J_d$ : $5.75\times10^{-3}$ Kg-m² | $r_g$ : 0.047 m |
| $m_m$ : 9.2 Kg | $m_p$ : 0.92 Kg |
| $m_d$ : 4.6 Kg | $m_g$ : 0.92 Kg |
| $I_p$ : $1.15\times10^{-3}$ Kg-m² | $k_{xx}, k_{yy}$ : variable |
| $I_g$ : $1.15\times10^{-3}$ Kg-m² | $k_m$ : $2.0\times10^{8}$ N/m |
| $F_s$ : 2500 N | |

Table 3 Parameters of the system shown in Fig. 6

| | |
|---|---|
| $I_p$ : 0.0018 Kg-m² | $m_p$ : 1.84 Kg |
| $I_g$ : 0.0018 Kg-m² | $m_g$ : 1.84 Kg |
| $r_p$ : 0.0445 m | $e_t$ : $9.3\times10^{-6}$ m |
| $r_g$ : 0.0445 m | $k_m$ : $1.0\times10^{8}$ N/m |
| $k_{xx}, k_{yy}$ : variable | $N_p$ : 28 teeth |

geometric eccentricity $e_g$ and the mass unbalance $U_g$ ($e_t$, $e_p$, and $U_p$ are all zero) is shown in Fig. 3, along with the experimental results of Iida et al. (1980). Since no information is given about the damping values of the system, a modal damping of 0.02 has been used at each mode in the computations. As seen in Fig. 3, predictions from the analytical model show good correlation with the experimental results.

**Response due to Geometric Eccentricities, Mass Unbalances, Static Transmission Error, and Mesh Stiffness Variation.** As a second example, the system which was used by Neriya et al. (1985) was studied to investigate the effects of geometric eccentricities and mass unbalances of the gears on the forced response of the system. The natural frequencies, mode shapes, and the responses at both gear locations due to geometric eccentricities and mass unbalances of gears were almost identical to those which were documented by Neriya et al. (1985). The results of this analysis have not been included in this study since the gear eccentricities and unbalances excite the system at the shaft rotational frequencies as was shown in the first example. The contribution of such low frequency excitations on the generated gear noise is usually negligible when compared with those of high frequency excitations caused by the static transmission error and the mesh stiffness variations.

On the other hand, the system shown in Fig. 4 has been modeled to obtain the dynamic mesh force due to the static transmission error excitation of amplitude $e_t$ and frequency $N_p\omega_p$ representing the mesh stiffness variation. Dimensions of the rotors are shown in Fig. 4 and other system parameters are listed in Table 2. The bearings are assumed to be identical and geometric eccentricities and mass unbalances for gears are assumed to be zero, so that only excitation causing a forced response is the static transmission error excitation defined. Since the displacement input approximates the loaded static transmission error, the value of $e_t$ was taken as the amplitude of the loaded static transmission error. Figure 5 shows the variation of the ratio of dynamic to static mesh load with rotational speed for three different bearing compliances. The first two small peaks of Fig. 5 correspond to torsional modes of shafts and the third peak corresponds to the coupled lateral/torsional mode governed by the gear mesh.

As shown in Fig. 5, when the bearing stiffnesses are decreased, the dynamic force also decreases considerably because of a resulting decrease in the relative angular rotations of the two gears. Although the displacements in the $y$ direction increase slightly, they do not appreciably affect the dynamic force. In this example, a mesh damping corresponding to a

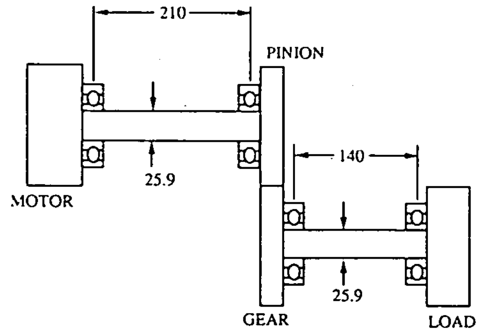


Fig. 4 The system of the second example (dimensions are in millimeters)

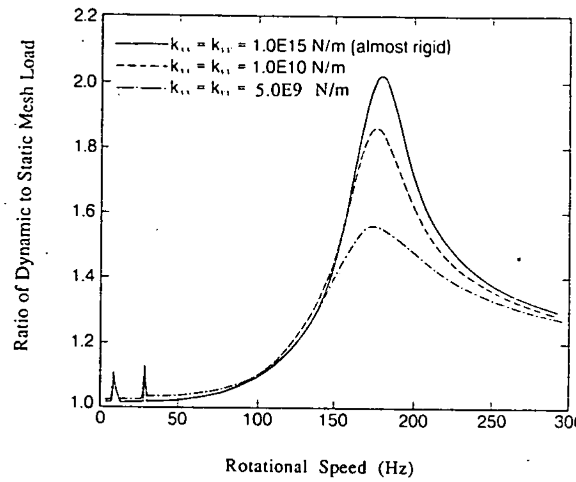


Fig. 5 Variation of dynamic to static load ratio with frequency for three different bearing compliances

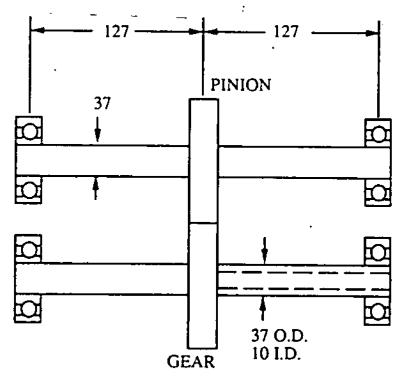


Fig. 6 The system analyzed as a third example (dimensions are in millimeters)

modal damping of 0.1 in the mode of gear mesh has been used. This was the value employed by several investigators for the same problem.

**The Effect of Bearing Compliances on Gear Dynamics.** A parametric study on the system shown in Fig. 6 was performed. The effects of bearing compliances on the natural frequencies and the forced response of the system to the harmonic excitation respresenting the static transmission error and the mesh stiffness variation were studied. The system parameters are given in Table 3. The natural frequencies and the physical descriptions of the corresponding modes for a value of bearing stiffnesses $k_{xx}=k_{yy}=1.0\times10^{9}$ N/m are presented in Table 4. The forced response at the pinion loca-

Table 4 First 14 natural frequencies of the system of Fig. 6 for the case of $k_{xx}/k_m = 10$

| Natural Frequency (Hz.) | Description of Corresponding Mode |
|---|---|
| 0 | torsional rigid body |
| 581 | transverse, torsional |
| 687 | transverse, x dir., driving shaft |
| 689 | transverse, y dir. |
| 691 | transverse, x dir., driven shaft |
| 2524 | transverse, torsional |
| 3387 | transverse, y dir. |
| 3387 | transverse, x dir., driving shaft |
| 3421 | transverse, x dir., driven shaft |
| 3421 | transverse, y dir. |
| 6447 | torsional, driving shaft |
| 6539 | torsional, driven shaft |
| 6831 | transverse, x dir., driving shaft |
| 6840 | transverse, y dir. |

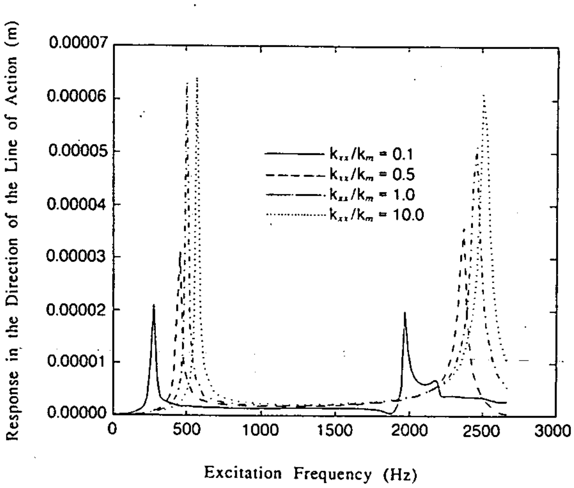


Fig. 7 Forced response of the system shown in Fig. 6 to the displacement excitation at the direction of pressure line (at pinion location) for four different bearing compliances

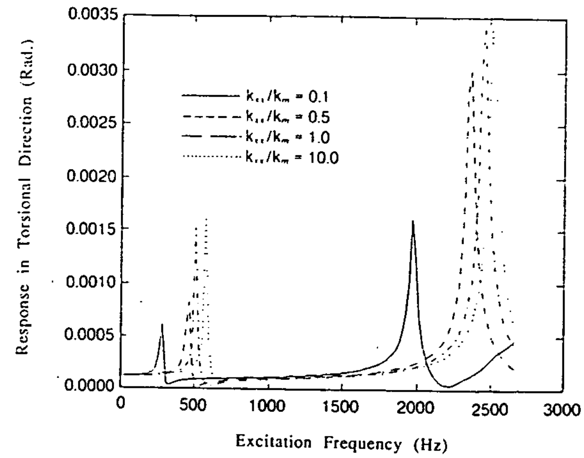


Fig. 8 Forced response of system shown in Fig. 6 to the displacement excitation at the torsional direction (at pinion location) for four different bearing compliances

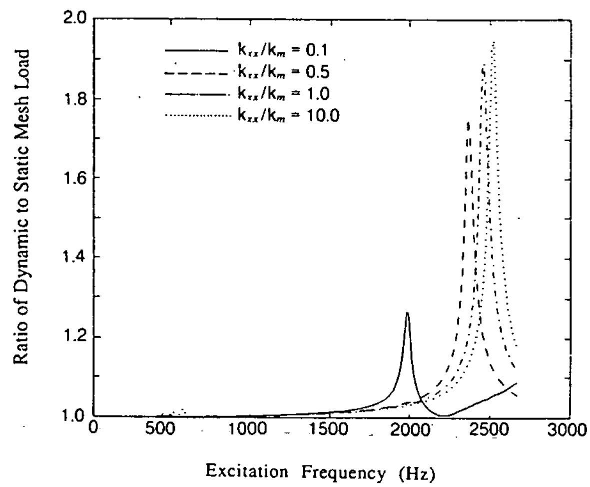


Fig. 9 Dynamic to static load ratios for system shown in Fig. 6 due to the displacement excitation for four different bearing compliances

tion in both the transverse (pressure line) and torsional directions, and dynamic mesh forces are plotted in Figs. 7, 8, and 9, respectively. As shown in Figs. 7 and 8, the system has peak responses only at two natural frequencies within the frequency range considered. Mode shapes corresponding to these two natural frequencies are presented in Fig. 10. If the free vibration characteristics of these two modes are investigated in detail, it is seen that the dynamic coupling between the transverse and torsional vibrations at these two modes are dominant. It is also seen that dynamic loads are high at only the second one of these two modes as shown in Fig. 9. The reason for this is that the transverse and torsional vibrations for the second mode considered are in phase. This results in large relative deflections at the mesh point which implies that this mode is governed by gear mesh. It is also seen from these figures that lowering the values of bearing stiffnesses causes a decrease in both the values of the natural frequencies and the amplitudes of the peak responses and dynamic loads.

Figure 11 shows the variation of these natural frequencies with bearing stiffnesses for three different shaft compliances: (*a*) long shafts (low stiffness) with dimensions given in Fig. 6, (*b*) moderately compliant shafts with half the length of case

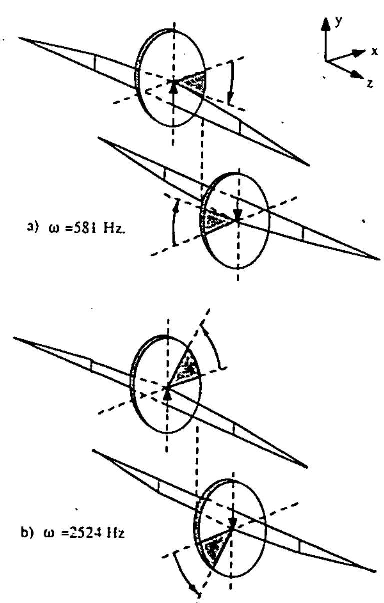


Fig. 10 Mode shapes corresponding to natural frequencies at which the system shown in Fig. 6 has peak responses

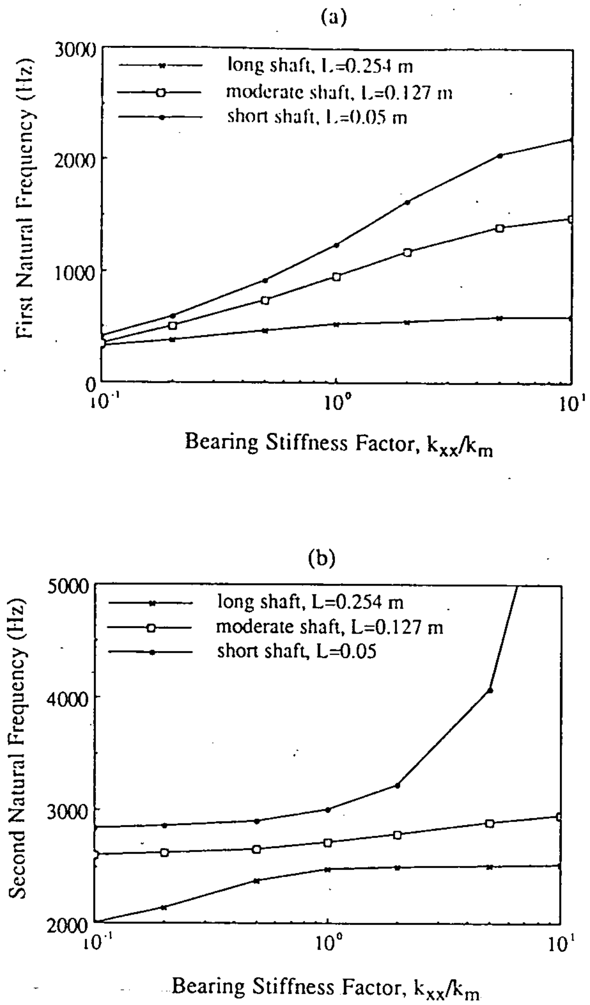


**Fig. 11 Variation of the first and the second natural frequencies considered with bearing stiffnesses for three different shaft compliances**

a, (*c*) very short (stiff) shafts. The shaft and the bearings supporting the gears can be thought of as two springs connected in series. When one of these components is very stiff compared to the other, its effect on the overall dynamic behavior becomes negligible. When the mode shapes for these two modes are examined for the case of short shafts and stiff bearings, the first of these two modes becomes purely torsional, while the lateral vibrations become more important in the second mode. As shown in Fig. 11(*a*), since the mode considered becomes purely torsional in the case of short shafts and stiff bearings, the value of this natural frequency does not change as bearing stiffnesses exceed a limiting value. For the other mode considered, the natural frequency becomes very high when a short shaft is used with a very stiff bearing, since the lateral vibrations are more dominant than torsional vibrations in this mode as shown in Fig. 11(*b*). Similarly, when the shafts are flexible enough the effect of bearing stiffnesses on the natural frequency becomes negligible above a limiting value of bearing stiffness.

## Conclusion

In this study, a finite element model to investigate the dynamic behavior of geared rotor systems has been developed. In the analysis, transverse and torsional vibrations of the shafts and the transverse vibrations of the bearings have been considered. The gear mesh was modeled by a pair of rigid disks connected by a spring and a damper with constant values which represent average mesh values. Tooth separation was not considered. The model developed yields the natural frequencies, corresponding mode shapes, and forced response of the system to the mass unbalances and the geometric eccentricities of gears and the transmission error.

Although a constant mesh stiffness was assumed, the self-excitation effect of a time-varying gear mesh was included into the analysis by using a displacement excitation representing the static transmission error. It may be justified to solve time-varying equations in simpler models with a few degrees of freedom. However, for large models such as the ones used in this study, avoiding time-varying stiffnesses and transient solutions saves considerable computation time. In the example problems only the first harmonic of the static transmission error was considered. A good correlation between the predictions and previous experimental and theoretical studies has been found.

Finally, it has been shown that the bearing compliances can greatly affect the dynamics of geared systems. Decreasing the stiffness values of bearings beyond a certain value lowers the natural frequency governed by the gear mesh considerably. However, in the case of compliant shafts, when the bearing stiffnesses are above a certain value the natural frequency corresponding to the gear mesh does not change considerably by increasing bearing stiffnesses. On the other hand, it has been seen that the amplitudes of dynamic to static load ratio and the deflections at the torsional and transverse directions are decreased by using bearings with higher compliances, which suggests that the bearing compliance may also affect the dynamic tooth load, depending upon the relative compliances of the other elements in the system.

## Acknowledgment

The authors would like to thank the sponsors of the Gear Dynamics and Gear Noise Research Laboratory and NASA Lewis Research Center (Grant No. NAG3-773) for providing advice and support of the research.

## References


Bagci, C., and Rajavenkateswaran, S. K., 1987, "Critical Speed and Modal Analyses of Rotating Machinery Using Spatial Finite-Line Element Method," *Proceedings of the Fifth International Modal Analysis Conference*, pp. 1708–1717.

Daws, J. W., 1979, "An Analytical Investigation of Three Dimensional Vibration in Gear-Coupled Rotor Systems," Ph.D. thesis, Virginia Polytechnic Institute and State University, Virginia.

Hagiwara, N., Iida, M., and Kikuchi, K., 1981, "Forced Vibration of a Pinion-Gear System Supported on Journal Bearings," *Proceedings of International Symposium of Gearing and Power Transmissions* (Tokyo), pp. 85–90.

Hamad, B. M., and Seireg, A., 1980, "Simulation of Whirl Interaction in Pinion-Gear Systems Supported on Oil Film Bearings," ASME *Journal of Engineering for Power*, Vol. 102, pp. 508–510.

Iida, H., Tamura, A., Kikuchi, K., and Agata, H., 1980, "Coupled Torsional-Flexural Vibration of a Shaft in a Geared System of Rotors (1st Report)," *Bulletin of Japanese Society of Mechanical Engineers*, Vol. 23, pp. 2111–2117.

Iida, H., and Tamura, A., 1984, "Coupled Torsional-Flexural Vibration of a Shaft in a Geared System," *Proceedings, Conference on Vibration in Rotating Machinery (Institution of Mechanical Engineers)*, pp. 67–72.

Iida, H., Tamura, A., and Oonishi, M., 1985, "Coupled Dynamic Characteristics of a Counter Shaft in a Gear Train System," *Bulletin of the Japanese Society of Mechanical Engineers*, Vol. 28, pp. 2694–2698.

Iida, H., Tamura, A., and Yamamoto, H., 1986, "Dynamic Characteristics of a Gear Train System with Softly Supported Shafts," *Bulletin of the Japanese Society of Mechanical Engineers*, Vol. 29, pp. 1811–1816.

Iwatsubo, N., Arii, S., and Kawai, R., 1984a, "Coupled Lateral-Torsional Vibrations of Rotor Systems Trained by Gears (1.Analysis by Transfer Matrix Method)," *Bulletin of the Japanese Society of Mechanical Engineers*, Vol. 27, pp. 271–277.

Iwatsubo, N., Arii, S., and Kawai, R., 1984b, "Coupled Lateral Torsional Vibration of a Geared Rotor System," *Proceedings of the Third International Conference on Vibrations in Rotating Machinery (Institution of Mechanical Engineers)*, pp. 59–66.

Lund, J. W., 1978, "Critical Speeds, Stability and Response of a Geared Train of Rotors," ASME JOURNAL OF MECHANICAL DESIGN, Vol. 100, pp. 535-538.

Mitchell, L. D., and David, J. W., 1985, "Proposed Solution Methodology for the Dynamically Coupled Nonlinear Geared Rotor Mechanics Equation," ASME *Journal of Vibration, Acoustics, Stress, and Reliability in Design*, Paper 85-DET-11.

Mitchell, L., and Mellen, D. M., 1975, "Torsional-Lateral Coupling in a Geared High-Speed Rotor System," *ASME Paper* 75-DET-75.

Nelson, H. D., 1980, "A Finite Rotating Shaft Element Using Timoshenko Beam Theory," ASME JOURNAL OF MECHANICAL DESIGN, Vol. 102, No. 4, pp. 793-803.

Nelson, H. D., and McVaugh, J. M., 1976, "The Dynamics of Rotor-Bearing Systems Using Finite Elements," ASME *Journal of Engineering for Industry*, Vol. 98, No. 2, pp. 593-600.

Neriya, S. V., Bhat, R. B., and Sankar, T. S., 1984, "Effect of Coupled Torsional-Flexural Vibration of a Geared Shaft System on Dynamic Tooth Load," *The Shock and Vibration Bulletin*, Part 3, Vol. 54, pp. 67-75.

Neriya, S. V., Bhat, R. B., and Sankar, T. S., 1985, "Coupled Torsional Flextural Vibration of a Geared Shaft System Using Finite Element Method," *The Shock and Vibration Bulletin*, Part 3, Vol. 55, pp. 13-25.

Ozguven, H. N., and Houser, D. R., 1988a, "Mathematical Models Used in Gear Dynamics-A Review," *Journal of Sound and Vibration*, Vol. 121, No. 3, pp. 383-411.

Ozguven, H. N., and Houser, D. R., 1988b, "Dynamic Analysis of High Speed Gears by Using Loaded Static Transmission Error," *Journal of Sound and Vibration*, Vol. 125, No. 1, pp. 71-83.

Ozguven, H. N., and Ozkan, Z. L., 1983, "Whirl Speeds and Unbalance Response of Multi-bearing Rotors Using Finite Elements," ASME *Journal of Vibration, Acoustics, Stress, and Reliability in Design*, Vol. 106, pp. 72-79.

Ozkan, Z. L., 1983, "Whirl Speeds and Unbalance Responses of Rotating Shafts Using Finite Elements," Ms. Thesis, The Middle East Technical University, Ankara, Turkey.

Zorzi, E. S., and Nelson, H. D., 1977, "Finite Element Simulation of Rotor-Bearing Systems with Internal Damping," ASME *Journal of Engineering for Power*, Vol. 99, pp. 71-76.

# SPECIAL ANNOUNCEMENT

## HONORS AND AWARDS NOMINATIONS

The Design Engineering Division Honors and Awards Committee solicits nominations for the ASME Machine Design Award and the Design Division Leonardo da Vinci Award.

The Machine Design Award recognizes eminent achievement or distinguished service in the field of machine design, including application, research, development, or teaching of machine design.

The Leonardo da Vinci Award recognizes eminent achievement in the design or invention of a product which is universally recognized as an important advancement in machine design.

The committee solicits nominations of outstanding individuals who may be eligible for these awards. The committee will assist the nominator in the preparation of documentation for a prospective candidate and requests your recommendations by November 1, 1992. For additional information please contact:

Roland Maki, Chairman
ASME DED Honors & Awards
2525 28 Mile Rd.
Rochester, MI 48306
(313) 651-9722